

Peristaltic Flow of a Jeffrey Fluid with Variable Viscosity in an Asymmetric Channel

Sohail Nadeem and Noreen Sher Akbar

Department of Mathematics, Quaid-i-Azam University 45320, Islamabad 44000, Pakistan

Reprint requests to S. N.; E-mail: snqau@hotmail.com

Z. Naturforsch. **64a**, 713–722 (2009); received January 13, 2009 / revised May 2, 2009

In this article, we have considered incompressible Jeffrey fluids and studied the effects of variable viscosity in the form of a well-known Reynold's model of viscosity in an asymmetric channel. The fluid viscosity is assumed to vary as an exponential function of temperature. The governing fundamental equations are approximated under the assumption of long wavelength and low Reynold number. The governing momentum and energy equations are solved using regular perturbation in terms of a small viscosity parameter β to obtain the expressions for stream functions pressure rise and temperature field. Numerical results are obtained for different values of viscosity parameter β , channel width d , wave amplitude b , and Jeffrey parameter λ_1 . It is observed that the behaviour of the physical parameters λ_1 , β , and d on pressure rise versus flow rate is as follows: when we increase these parameters pressure rise decreases while pressure rise increases with the increase in b . It is also observed that temperature profile increases when we increase E_c , P_r , and β . Trapping phenomena are also discussed at the end of the article to see the behaviour of different parameters on streamlines.

Key words: Peristaltic Flow; Jeffrey Fluid; Variable Viscosity; Heat Transfer; Reynold's Model.

1. Introduction

Heat transfer analysis in two-dimensional flows have attracted the attention of a number of researchers in the last few decades due to its applications. These heat transfer applications include transport of water from the ground to the upper branches of a tree, glass fiber production, metal extrusion, hot rolling, wire drawing, paper production, drawing of plastic films, metal and polymer extraction, metal spinning, etc.

Peristalsis is a suitable process for a fluid transport that is used by many systems to propel or to mix the contents of a tube. Some applications of the peristaltic transport include, urine transport from kidney to bladder, swallowing food through the esophagus, chyme motion in the gastrointestinal tract, vasomotion of small blood vessels, and movement of spermatozoa in human reproductive tract. Some important studies dealing with the peristaltic flow are discussed in [1–6]. The study of heat transfer in connection with peristaltic motion has industrial and biological applications such as sanitary fluid transport, blood pumps in heart lungs machine, and transport of corrosive fluids where the contact of the fluid with machinery parts is prohibited. The effect of heat transfer on the peristaltic flow of an electrically conducting fluid in a porous space

is studied by Hayat et al. [7]. The effects of elasticity of the flexible walls on the peristaltic transport of viscous fluid with heat transfer in a two-dimensional uniform channel have been investigated by Radhakrishnamacharya and Srinivasulu [8]. Vajravelu et al. [9] have discussed the interaction of peristalsis with heat transfer for the flow of a viscous fluid in a vertical porous annulus region between two concentric tubes. They concluded that for the large values of amplitude ratio, the effects of pressure rise on the flow rate is negligible. The attention of peristaltic and heat transfer has been recognized and has received some attention [10–20] as it is thought to be relevant in some important processes such as hemodialysis and oxygenation.

In most of the above mentioned studies, the fluid viscosity is assumed to be constant. This assumption is not valid everywhere. In general the coefficient of viscosity for real fluids are functions of temperature and pressure. For many liquids such as water, oils, and blood, the variation of viscosity due to temperature change is more dominant than other effects. The pressure dependence viscosity is usually very small and can be neglected. All of the above mentioned studies adopt the assumption of constant viscosity in order to simplify the calculations. Infact, in many thermal transport processes, the temperature distribution within

the flow field is never uniform, i. e. the fluid viscosity changes noticeably if a large temperature difference exists in a system. Therefore, it is highly desirable to include the effect of temperature dependent viscosity in momentum and thermal transport processes [21-25].

Considering the importance of heat transfer in peristalsis and keeping in mind the sensitivity of liquid viscosity to temperature, an attempt is made to study the effect of heat transfer in peristaltic flow of Jeffrey fluid in an asymmetric channel with variable temperature dependent viscosity. To the best of authors knowledge, no attempt has been made to study the effects of variable viscosity in Jeffrey fluid. We use an exponential form of viscosity temperature relation known as Reynold’s model. The non-dimensional problem is formulated in the wave frame under the long wavelength and low Reynolds number approximations. By using regular perturbation method, asymptotic solutions for stream function, temperature, and pressure rise are obtained. In order to study the quantitative effects, graphical results are presented and discussed for different physical quantities. We investigate the effects of variable viscosity on the behaviour of the pressure drop, pressure rise, and temperature profiles. The results are presented and analyzed for an adequate range of parameters.

2. Mathematical Formulation

We consider an incompressible Jeffrey fluid in an asymmetric channel. The lower wall of the channel is maintained at temperature T_1 while the upper wall has temperature T_0 . Since we are considering an asymmetric channel, the channel flow is produced due to different amplitudes and phases of the peristaltic waves on the channel.

The geometry of the wall surface is defined as

$$\begin{aligned}
 Y = H_1 &= d_1 + a_1 \sin \left[\frac{2\pi}{\lambda} (X - ct) \right], \\
 Y = H_2 &= -d_2 - b_1 \sin \left[\frac{2\pi}{\lambda} (X - ct) + \phi \right],
 \end{aligned}
 \tag{1}$$

where a_1 and b_1 are the amplitudes of the waves, λ is the wave length, $d_1 + d_2$ is the width of the channel, c is the velocity of propagation, t is the time, and X is the direction of wave propagation. The phase difference ϕ varies in the range $0 \leq \phi \leq \pi$ in which $\phi = 0$ corresponds to a symmetric channel with waves out of phase and $\phi = \pi$ means that the waves are in phase.

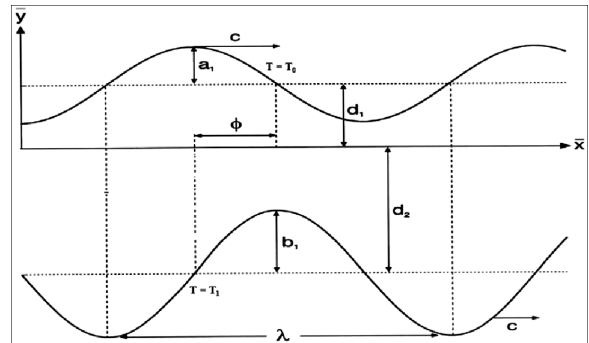


Illustration. Geometry of the Problem.

Further, $a_1, b_1, d_1, d_2,$ and ϕ satisfy the condition

$$a_1^2 + b_1^2 + 2a_1b_1 \cos \phi \leq (d_1 + d_2)^2.$$

The equations governing the flow of a Jeffrey fluid are given by

$$\begin{aligned}
 \frac{\partial U}{\partial X} + \frac{\partial V}{\partial Y} &= 0, \\
 \rho \left(\frac{\partial U}{\partial t} + U \frac{\partial U}{\partial X} + V \frac{\partial U}{\partial Y} \right) &= \\
 - \frac{\partial P}{\partial X} + \frac{\partial}{\partial X} (S_{XX}) + \frac{\partial}{\partial Y} (S_{XY}), & \\
 \rho \left(\frac{\partial V}{\partial t} + U \frac{\partial V}{\partial X} + V \frac{\partial V}{\partial Y} \right) &= \\
 - \frac{\partial P}{\partial Y} + \frac{\partial}{\partial X} (S_{YX}) + \frac{\partial}{\partial Y} (S_{YY}), & \\
 C' \left(\frac{\partial T}{\partial t} + U \frac{\partial T}{\partial X} + V \frac{\partial T}{\partial Y} \right) &= \frac{K'}{\rho} \nabla^2 T + v \Phi,
 \end{aligned}
 \tag{2}$$

where

$$\begin{aligned}
 \nabla^2 &= \frac{\partial^2}{\partial X^2} + \frac{\partial^2}{\partial Y^2}, \\
 \Phi &= \frac{\mu(T)}{1 + \lambda_1} \left[1 + \lambda_2 \left(U \frac{\partial}{\partial X} + V \frac{\partial}{\partial Y} \right) \right] \\
 &\cdot \left[2 \left(\frac{\partial U}{\partial X} \right)^2 + 2 \left(\frac{\partial V}{\partial Y} \right)^2 + \left(\frac{\partial U}{\partial Y} + \frac{\partial V}{\partial X} \right)^2 \right].
 \end{aligned}$$

U, V are the velocities in X - and Y -directions in a fixed frame, ρ is the constant density, P is the pressure, σ is the electrical conductivity, K' is the thermal conductivity, C' is the specific heat, and T is the temperature.

The constitutive equation for the extra stress tensor S where for a Jeffrey fluid is defined by [2]

$$S = \frac{\mu(T)}{1 + \lambda_1} (\dot{\gamma} + \lambda_2 \ddot{\gamma}). \tag{3}$$

Here $\mu(T)$ is the temperature dependent viscosity, λ_1 is the ratio of relaxation to retardation times, $\dot{\gamma}$ the shear rate, λ_2 the retardation time, and dots denote the differentiation with respect to time.

We introduce a wave frame (x, y) moving with velocity c away from the fixed frame (X, Y) by the transformation

$$x = X - ct, \quad y = Y, \quad u = U - c, \quad v = V, \tag{4}$$

and $p(x) = P(X, t)$.

Defining

$$\begin{aligned} \bar{x} &= \frac{2\pi x}{\lambda}, \quad \bar{y} = \frac{y}{d_1}, \quad \bar{u} = \frac{u}{c}, \quad \bar{v} = \frac{v}{c\delta}, \\ \delta &= \frac{d_1}{\lambda}, \quad d = \frac{d_2}{d_1}, \quad \bar{p} = \frac{d_1^2 p}{\mu_0 c \lambda}, \quad \bar{t} = \frac{ct}{\lambda}, \\ h_1 &= \frac{H_1}{d_1}, \quad h_2 = \frac{H_2}{d_2}, \quad a = \frac{a_1}{d_1}, \quad b = \frac{b_1}{d_1}, \\ R_e &= \frac{cd_1}{\nu}, \quad \bar{\Psi} = \frac{\Psi}{cd_1}, \quad \theta = \frac{T - T_0}{T_1 - T_0}, \\ E_c &= \frac{c^2}{C'(T_1 - T_0)}, \quad P_r = \frac{\rho \nu C'}{K'}, \quad \bar{S} = \frac{Sd_1}{\mu_0 c}, \\ \mu(\theta) &= \frac{\mu(T)}{\mu_0}. \end{aligned} \tag{5}$$

Using the above non-dimensional quantities, the resulting equations in terms of a stream function Ψ (dropping the bars and setting $u = \frac{\partial \Psi}{\partial y}$, $v = -\frac{\partial \Psi}{\partial x}$) can be written as

$$R_e \delta [\Psi_y \Psi_{xy} - \Psi_x \Psi_{yy}] = -\frac{\partial p}{\partial x} + \delta \frac{\partial}{\partial x} (S_{xx}) + \frac{\partial}{\partial y} (S_{xy}), \tag{6}$$

$$R_e \delta^3 [-\Psi_y \Psi_{xx} + \Psi_x \Psi_{xy}] = -\frac{\partial p}{\partial y} + \delta^2 \frac{\partial}{\partial x} (S_{yx}) + \delta \frac{\partial}{\partial y} (S_{yy}), \tag{7}$$

$$\begin{aligned} R_e \delta [\Psi_y \theta_x - \Psi_x \theta_y] &= \frac{1}{P_r} [\theta_{yy} + \delta^2 \theta_{xx}] \\ &+ \frac{E_c \mu(\theta)}{(1 + \lambda_1)} \left[1 + \frac{\lambda_2 c \delta}{d_1} \left(\Psi_y \frac{\partial}{\partial x} - \Psi_x \frac{\partial}{\partial y} \right) \right] \\ &\cdot [4\delta^2 \Psi_{xy}^2 + (\Psi_{yy} - \delta^2 \Psi_{xx})^2], \end{aligned} \tag{8}$$

$$\begin{aligned} S_{xx} &= \frac{2\mu(\theta)\delta}{1 + \lambda_1} \left[1 + \frac{\lambda_2 c \delta}{d_1} \left(\Psi_y \frac{\partial}{\partial x} - \Psi_x \frac{\partial}{\partial y} \right) \right] \Psi_{xy}, \\ S_{xy} &= \frac{\mu(\theta)}{1 + \lambda_1} \left[1 + \frac{\lambda_2 c \delta}{d_1} \left(\Psi_y \frac{\partial}{\partial x} - \Psi_x \frac{\partial}{\partial y} \right) \right] [\Psi_{yy} - \delta^2 \Psi_{xx}], \\ S_{yy} &= -\frac{2\mu(\theta)\delta}{1 + \lambda_1} \left[1 + \frac{\lambda_2 c \delta}{d_1} \left(\Psi_y \frac{\partial}{\partial x} - \Psi_x \frac{\partial}{\partial y} \right) \right] \Psi_{xy}. \end{aligned}$$

The corresponding boundary conditions are

$$\begin{aligned} \Psi &= \frac{q}{2}, \quad \text{at } y = h_1 = 1 + a \sin x, \\ \Psi &= -\frac{q}{2}, \quad \text{at } y = h_2 = -d - b \sin(x + \phi), \\ \frac{\partial \Psi}{\partial y} &= -1, \quad \text{at } y = h_1 \quad \text{and } y = h_2, \\ \theta &= 0, \quad \text{at } y = h_1, \\ \theta &= 1, \quad \text{at } y = h_2, \end{aligned} \tag{9}$$

where q is the flux in the wave frame and a, b, ϕ , and d satisfy the relation

$$a^2 + b^2 + 2ab \cos \phi \leq (1 + d)^2.$$

Under the assumption of long wave length $\delta \ll 1$ and low Reynold number and neglecting the terms of order δ and higher, (6) to (8) take the form

$$0 = -\frac{\partial p}{\partial x} + \frac{\partial}{\partial y} \left[\frac{\mu(\theta)}{1 + \lambda_1} \frac{\partial^2 \Psi}{\partial y^2} \right], \tag{10}$$

$$0 = -\frac{\partial p}{\partial y}, \tag{11}$$

$$0 = \frac{1}{P_r} \frac{\partial^2 \theta}{\partial y^2} + \frac{E_c \mu(\theta)}{(1 + \lambda_1)} \left(\frac{\partial^2 \Psi}{\partial y^2} \right)^2. \tag{12}$$

Elimination of pressure from (10) and (11) yields

$$\frac{\partial^2}{\partial y^2} \left[\frac{\mu(\theta)}{1 + \lambda_1} \frac{\partial^2 \Psi}{\partial y^2} \right] = 0, \tag{13}$$

$$\frac{1}{P_r} \frac{\partial^2 \theta}{\partial y^2} + \frac{E_c \mu(\theta)}{(1 + \lambda_1)} \left(\frac{\partial^2 \Psi}{\partial y^2} \right)^2 = 0. \tag{14}$$

The flux at any axial station in the fixed frame is

$$\begin{aligned} \bar{Q} &= \int_{h_2}^{h_1} (u + 1) dy \\ &= \int_{h_2}^{h_1} u dy + \int_{h_2}^{h_1} dy = q + h_1 - h_2. \end{aligned} \tag{15}$$

The average volume flow rate over one period ($T = \frac{\lambda}{c}$) of the peristaltic wave is defined as

$$Q = \frac{1}{T} \int_0^T \bar{Q} dt = \frac{1}{T} \int_0^T (q + h_1 - h_2) dt = q + 1 + d. \tag{16}$$

3. Reynold’s Viscosity Model

The Reynold’s model viscosity is defined as

$$\mu(\theta) = e^{-\beta\theta}, \tag{17}$$

where β is constant.

The Maclaurin’s series expansion of the above equation can be written as

$$\mu(\theta) = 1 - \beta\theta + O(\beta)^2. \tag{18}$$

With the help of (18), Eqs. (13) and (14) take the form

$$\frac{\partial^2}{\partial y^2} \left[\frac{(1 - \beta\theta)}{1 + \lambda_1} \frac{\partial^2 \Psi}{\partial y^2} \right] = 0, \tag{19}$$

$$\frac{\partial^2 \theta}{\partial y^2} + \frac{(1 - \beta\theta)P_r E_c}{(1 + \lambda_1)} \left(\frac{\partial^2 \Psi}{\partial y^2} \right)^2 = 0. \tag{20}$$

4. Solution of the Problem

Equations (19) and (20) are coupled nonlinear differential equations. The exact solutions of these equations are not possible, therefore they had to be obtained by using the regular perturbation method considering the viscosity parameter to be $\beta \ll 1$.

The expression for the stream function and temperature profile satisfying boundary condition can be directly written as (see Appendix):

$$\Psi = \frac{(1 + \lambda_1)L_1 y^3}{6} + \frac{(1 + \lambda_1)L_2 y^2}{2} + L_3 y + L_4 + \beta(L_{21} y^7 + L_{22} y^6 + L_{23} y^5 + L_{24} y^4 + L_{31} y^3 + L_{32} y^2 + L_{29} y + L_{30}), \tag{21}$$

$$\theta = L_{10} y^4 + L_{11} y^3 + L_{12} y^2 + L_{13} y + L_{14} + \beta(R_{12} y^{12} + R_{13} y^{11} + R_{14} y^{10} + R_{15} y^9 + R_{16} y^8 + R_{17} y^7 + R_{18} y^6 + R_{19} y^5 + R_{20} y^4 + R_{21} y^3 + R_{22} y^2 + R_{25} y + R_{26}). \tag{22}$$

The axial pressure gradient can be written as:

$$\frac{dp}{dx} = -\frac{12(h_1 - h_2 + q)}{(h_1 - h_2)^3(1 + \lambda_1)} + \frac{6\beta}{7(h_1 - h_2)^5(1 + \lambda_1)} \cdot [(h_1 - h_2)^3 R_{27} + (h_1 - h_2)^2 R_{28} + 18(h_1 - h_2)R_{29} + R_{30}]. \tag{23}$$

The pressure rise Δp_λ is given by

$$\Delta p_\lambda = \int_0^1 \left(\frac{dp}{dx} \right) dx. \tag{24}$$

where $\frac{dp}{dx}$ is defined in (24).

5. Graphical Results and Discussion

To discuss the effects of various parameters involved in the problem such as viscosity parameter β , Jeffrey parameter λ_1 , channel widths d , wave amplitude b , Prandtl number P_r , and Eckert number E_c on the solution of the problem numerical results are calculated and can be analyzed through the following figures. Figures 1–4 illustrate the pressure rise against flow rate for several values of β , λ_1 , b , and d . It is seen from Figure 1 that the maximum pressure rise occurs at zero flow rate for different values of β and pressure rise decreases by increasing β in the region $\Theta \in [-1.5, 0.2]$, which is known as peristaltic pumping region, and in the region $\Theta \in [0.21, 1.5]$, pressure rise increases by increasing β which is the augmented pumping region. In Figure 2, we have discussed the effects of b on the pressure rise Δp_λ . It is analyzed, that with increasing b , pressure rise increases in the region $\Theta \in [-1.5, 0.8]$, otherwise the pressure rise decreases with the increase in b in the region $\Theta \in [0.81, 1.5]$. The first region denotes the peristaltic pumping region ($\Delta p_\lambda > 0, \Theta > 0$) and the second region is known as augmented pumping region ($\Delta p_\lambda < 0, \Theta > 0$).

Figure 3 shows the effects of d on the average pressure rise Δp_λ . It is depicted that the pressure rise decreases with the increase in d in the region $\Theta \in [-1.5, 0.4]$ ($\Delta p_\lambda > 0, \Theta > 0$, peristaltic pumping region), the pressure rise increases with the increase in d in the region $\Theta \in [0.41, 1.5]$ ($\Delta p_\lambda < 0, \Theta > 0$, augmented pumping region). The effects of Jeffrey parameter λ_1 can be analyzed through Figure 4. It is observed that the pressure rise decreases with the increase in λ_1 in the region $\Theta \in [-1.5, 0.2]$ ($\Delta p_\lambda > 0, \Theta > 0$, peristaltic pumping region), the pressure

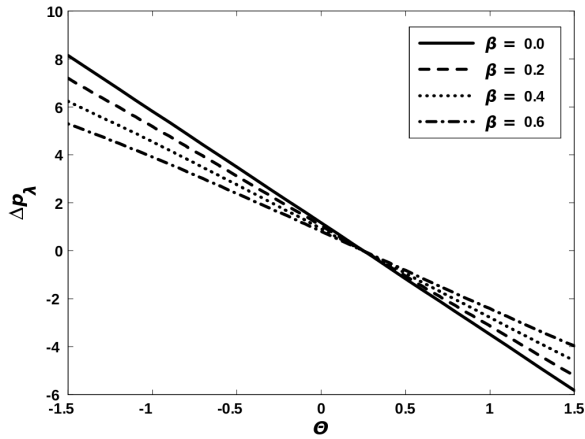


Fig. 1. Pressure rise versus flow rate for $E_c = 0.2$, $P_r = 0.3$, $a = 0.2$, $b = 0.3$, $d = 0.4$, $\phi = 0.2$, and $\lambda_1 = 0.4$.

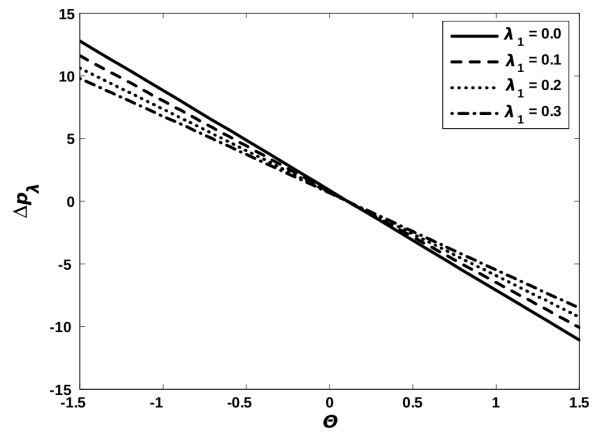


Fig. 4. Pressure rise versus flow rate for $E_c = 0.3$, $P_r = 0.3$, $a = 0.2$, $b = 0.3$, $d = 0.4$, $\phi = 0.1$, and $\beta = 0.1$.

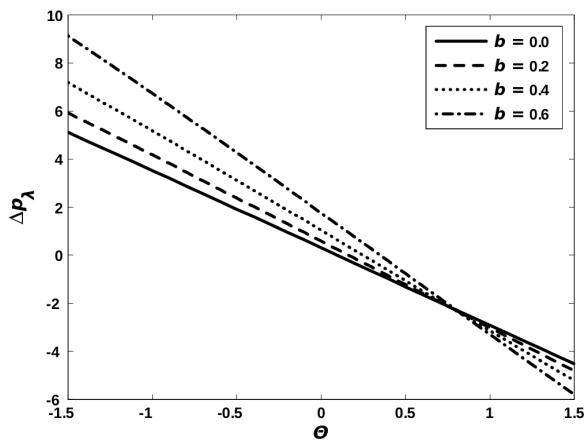


Fig. 2. Pressure rise versus flow rate for $E_c = 0.2$, $P_r = 0.3$, $a = 0.2$, $\beta = 0.2$, $d = 0.4$, $\phi = 0.2$, and $\lambda_1 = 0.4$.

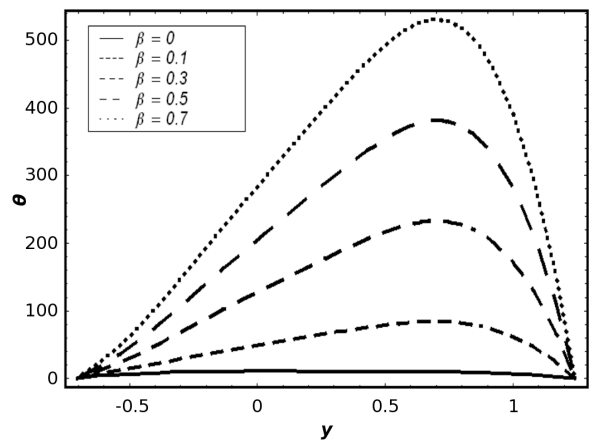


Fig. 5. Temperature profile for $E_c = 3$, $P_r = 3$, $a = 0.3$, $b = 0.3$, $d = 0.5$, $\phi = 0.2$, $q = 0.4$, $\lambda_1 = 0.2$, and $x = 0.1$.

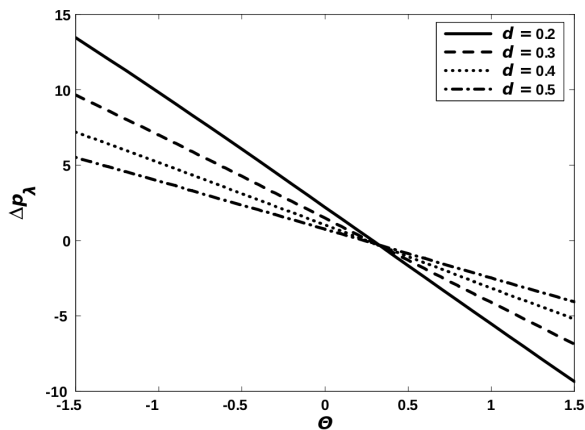


Fig. 3. Pressure rise versus flow rate for $E_c = 0.3$, $P_r = 0.3$, $a = 0.2$, $b = 0.3$, $\beta = 0.2$, $\phi = 0.2$, and $\lambda_1 = 0.4$.

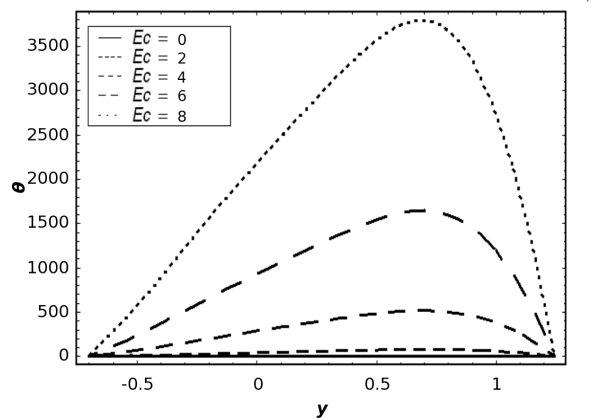


Fig. 6. Temperature profile for $\beta = 0.3$, $P_r = 3$, $a = 0.3$, $b = 0.3$, $d = 0.5$, $\phi = 0.2$, $q = 0.4$, $\lambda_1 = 0.2$, and $x = 0.1$.

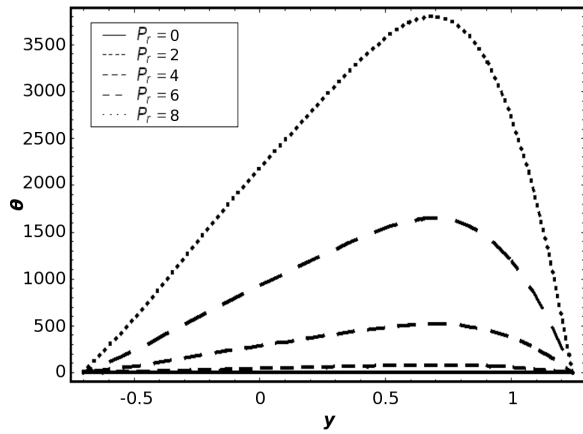


Fig. 7. Temperature profile for $E_c = 3$, $\beta = 0.3$, $a = 0.3$, $b = 0.3$, $d = 0.5$, $\phi = 0.2$, $q = 0.4$, $\lambda_1 = 0.2$, and $x = 0.1$.

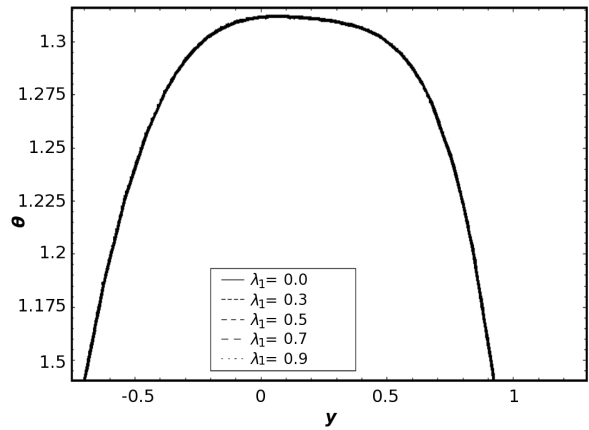


Fig. 8. Temperature profile for $E_c = 3$, $\beta = 0.3$, $a = 0.5$, $b = 0.5$, $d = 0.5$, $\phi = 0.1$, $q = 0.4$, $P_r = 0.2$, and $x = 0.1$.

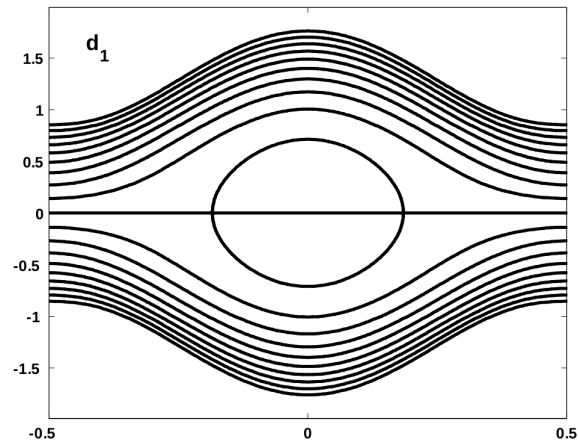
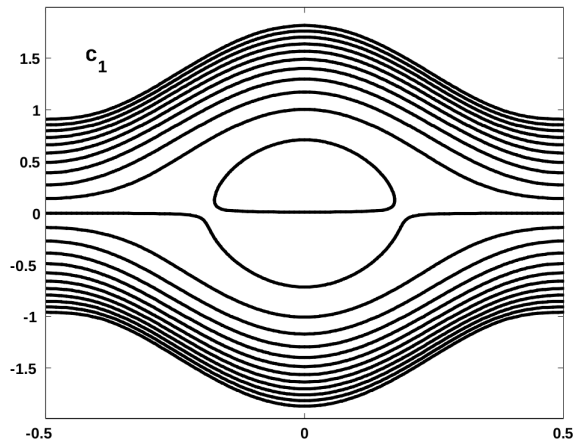
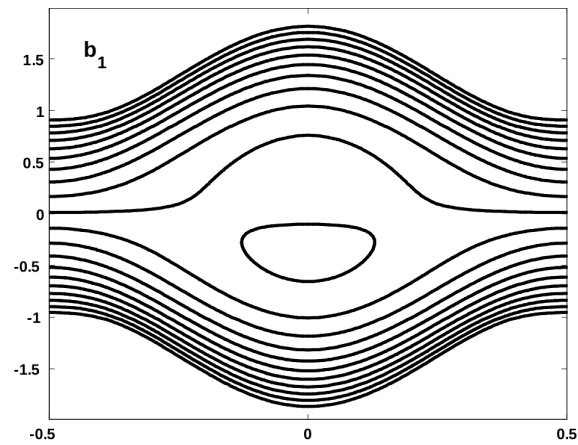
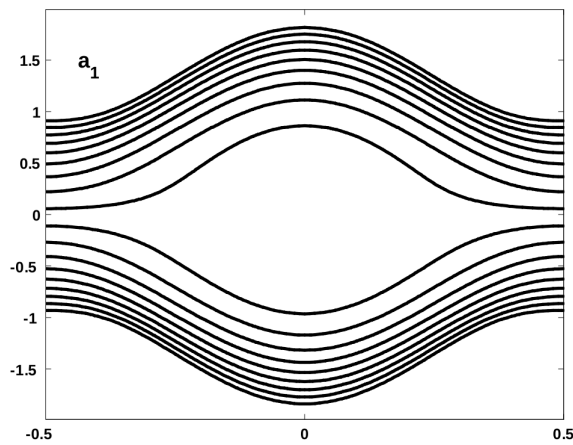


Fig. 9. Streamlines for different values of $\Theta = 1.2, 1.3, 1.4, 1.5$ (panels a_1 to d_1). The other parameters are: $E_c = 0.1$, $P_r = 0.1$, $a = 0.5$, $b = 0.5$, $d = 1$, $\phi = 0.0$, $\lambda_1 = 0.2$, and $\beta = 0.1$.

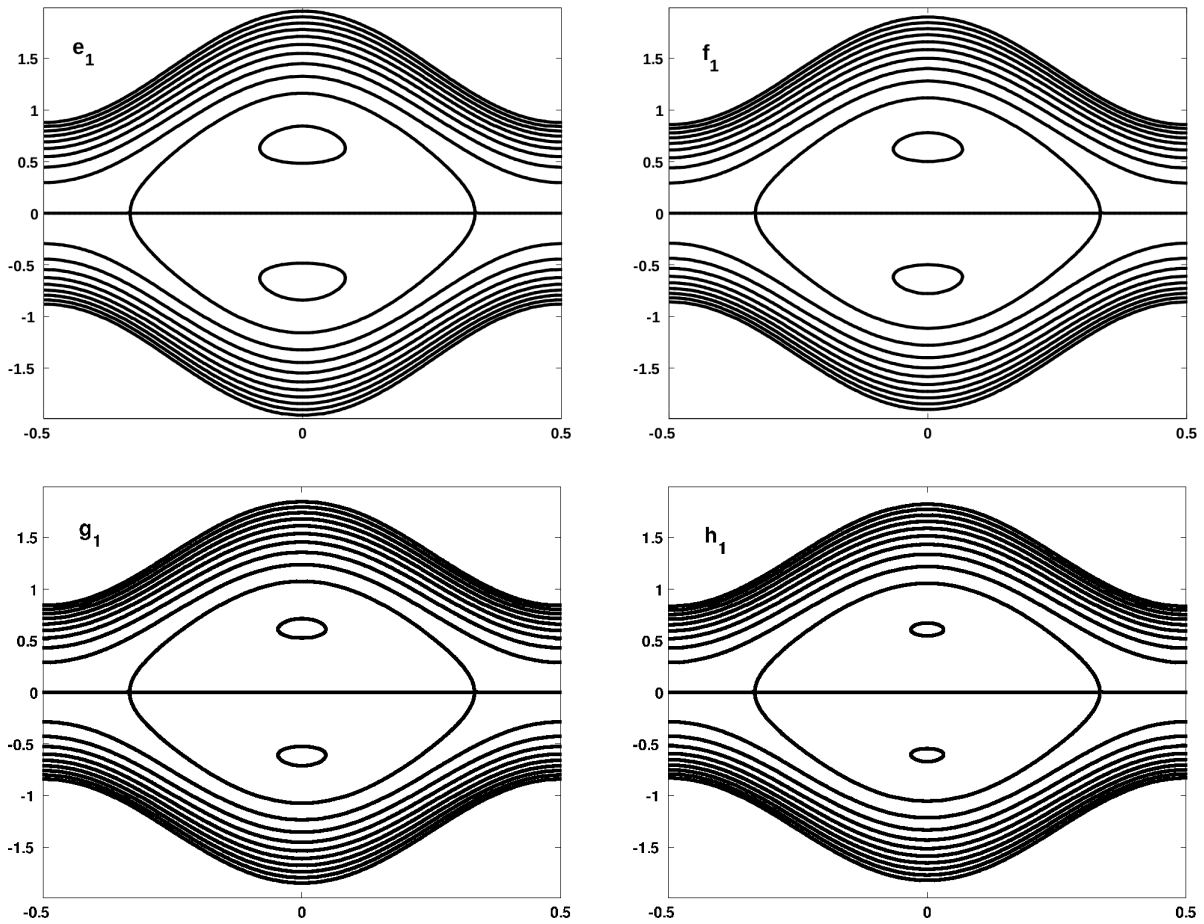


Fig. 10. Streamlines for different values of $\lambda_1 = 0.1, 0.2, 0.3, 0.4$ (panels e_1 to h_1). The other parameters are: $E_c = 0.1, P_r = 0.1, a = 0.5, b = 0.5, d = 1, \phi = 0.0$, and $\beta = 0.2$.

rise increases with the increase in λ_1 in the region $\Theta \in [0.21, 1.5]$ ($\Delta p_\lambda < 0, \Theta > 0$, augmented pumping region).

The temperature profile for different values of β, λ_1, P_r , and E_c are plotted in Figures 5–8. It is observed from the figures that the increase in β, E_c , and P_r the temperature profile increases. The temperature profile for different values of λ_1 is plotted in Figure 8, the graph overlapped for different values of λ_1 .

Trapping is another interesting phenomenon in peristaltic motion. It is basically the formation of an in-

ternally circulating bolus of fluid by closed streamlines. This trapped bolus pushed a head along with the peristaltic wave. Figure 9 illustrate the streamline graphs for different values of time mean flow rate Θ . It is observed that with the increase in Θ trapped bolus enclosed. The streamlines for different values λ_1 are shown in Figure 10. It is evident from the figure that the size of the trapped bolus decreases by increasing λ_1 . The streamlines for different values of β are shown in Figure 11. It is observed that with the increase in β , the size trapped bolus decreases.

Appendix

$$L_1 = -\frac{12(h_1 - h_2 + q_0)}{(h_1 - h_2)^3(1 + \lambda_1)}, \quad L_2 = \frac{6(h_1^2 - h_2^2 + (h_1 + h_2)q_0)}{(h_1 - h_2)^3(1 + \lambda_1)}, \quad L_3 = -\frac{(h_1^3 - h_2^3) + 3h_1h_2(h_1 - h_2) + 6h_1h_2q_0}{(h_1 - h_2)^3},$$

$$L_4 = \frac{(h_1 + h_2)(2h_1h_2(h_1 - h_2) - (h_1^2 - 4h_1h_2 + h_2^2)q_0)}{2(h_1 - h_2)^3}, \quad L_5 = (1 + \lambda_1)L_1, \quad L_6 = (1 + \lambda_1)L_2,$$

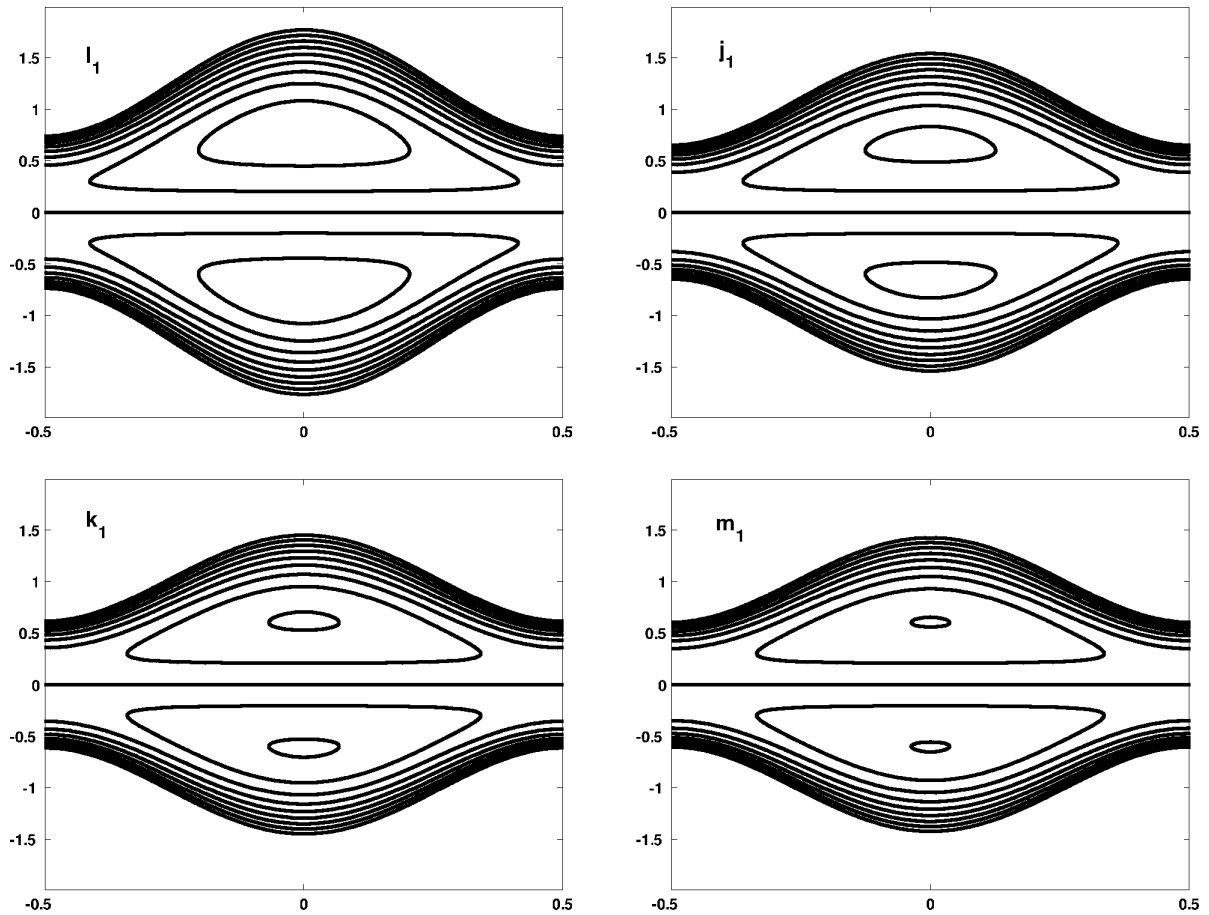


Fig. 11. Streamlines for different values of $\beta = 0.1, 0.2, 0.3, 0.4$ (panels l_1 to m_1). The other parameters are $E_c = 0.1, P_r = 0.1, a = 0.5, b = 0.5, d = 1, \phi = 0.0$, and $\lambda_1 = 0.2$.

$$\begin{aligned}
 L_7 &= -E_c P_r L_5^2, & L_8 &= -2E_c P_r L_5 L_6, & L_9 &= -E_c P_r L_6^2, & L_{10} &= \frac{L_7}{12}, & L_{11} &= \frac{L_8}{6}, & L_{12} &= \frac{L_9}{2}, \\
 L_{13} &= \frac{1}{(h_1 - h_2)} (1 + L_{10}(h_1^4 - h_2^4) + L_{11}(h_1^3 - h_2^3) + L_{12}(h_1^2 - h_2^2)), & L_{14} &= -L_{10}h_1^4 - L_{11}h_1^3 - L_{12}h_1^2 - L_{13}h_1, \\
 L_{15} &= L_{10}L_5, & L_{16} &= L_{11}L_5 + L_{10}L_6, & L_{17} &= L_{12}L_5 + L_{11}L_6, & L_{18} &= L_{13}L_5 + L_{12}L_6, & L_{19} &= L_{14}L_5 + L_{13}L_6, \\
 L_{20} &= L_{14}L_6, & L_{21} &= \frac{L_{15}}{42}, & L_{22} &= \frac{L_{16}}{30}, & L_{23} &= \frac{L_{17}}{20}, & L_{24} &= \frac{L_{18}}{12}, & L_{25} &= \frac{L_{19}}{6}, & L_{26} &= \frac{L_{20}}{2}, \\
 L_{27} &= -\frac{12(h_1 - h_2 + q_1)}{(h_1 - h_2)^3(1 + \lambda_1)} + \frac{6((h_1 - h_2)^3 R_{27} + (h_1 - h_2)^2 R_{28} + 18(h_1 - h_2) R_{29} + R_{30})}{7(h_1 - h_2)^5(1 + \lambda_1)} \\
 L_{28} &= \frac{1}{(h_1 - h_2)^3(1 + \lambda_1)} (2((h_1 - h_2)^3(4h_1^5 L_{21} + h_1^4(16h_2 L_{21} + 3L_{22}) + 2h_1^3(11h_2^2 L_{21} + 6h_2 L_{22} + L_{23})) \\
 &\quad + 4h_1 h_2(4h_2^3 L_{21} + 3h_2^2 L_{22} + 2h_2 L_{23} + L_{24}) + h_2^2(4h_2^3 L_{21} + 3h_2^2 L_{22} + 2h_2 L_{23} + L_{24}) \\
 &\quad + h_1^2(22h_2^3 L_{21} + 15h_2^2 L_{22} + 8h_2 L_{23} + L_{24}) - L_{26}) + 3(h_1 + h_2)q_1), \\
 L_{29} &= -\frac{1}{(h_1 - h_2)^3} (h_1 h_2((h_1 - h_2)^3(8h_1^4 L_{21} + h_1^3(17h_2 L_{21} + 6L_{22}) + 4h_1^2(5h_2^2 L_{21} + 3h_2 L_{22} + L_{23}) \\
 &\quad + 2h_2(4h_2^3 L_{21} + 3h_2^2 L_{22} + 2h_2 L_{23} + L_{24}) + h_1(17h_2^3 L_{21} + 17h_2^2 L_{22} + 7h_2 L_{23} + 2L_{24})) + 6q_1),
 \end{aligned}$$

$$\begin{aligned}
L_{30} &= h_1^2 h_2^2 (4h_1^3 L_{21} + 4h_2^3 L_{21} + 3h_2^2 L_{22} + 3h_1^2 (2h_2 L_{21} + L_{22})) + 2h_2 L_{23} + 2h_1 (3h_2^2 L_{21} + 2h_2 L_{22} + L_{23}) \\
&\quad + L_{24} - \frac{(h_1 + h_2)(h_1^2 - 4h_1 h_2 + h_2^2) q_1}{2(h_1 - h_2)^3}, \\
L_{31} &= L_{25} + \frac{L_{27}}{6} (1 + \lambda_1), \quad L_{32} = L_{26} + \frac{L_{28}}{2} (1 + \lambda_1), \quad L_{33} = 6L_{31}, \quad L_{34} = 2L_{32}, \quad L_{35} = L_{15}^2, \\
L_{36} &= 2L_{15} L_{16}, \quad L_{37} = 2L_{15} L_{17} + L_{16}^2, \quad L_{38} = 2L_{15} L_{18} + 2L_{16} L_{17}, \quad L_{39} = 2L_{15} L_{33} + 2L_{16} L_{18} + L_{17}^2, \\
L_{40} &= 2L_{15} L_{34} + 2L_{16} L_{33} + 2L_{17} L_{18}, \quad L_{41} = 2L_{16} L_{34} + 2L_{17} L_{33} + L_{18}^2, \quad L_{42} = 2L_{17} L_{34} + 2L_{18} L_{33}, \\
L_{43} &= 2L_{18} L_{34} + L_{33}^2, \quad L_{44} = 2L_{33} L_{34}, \quad L_{45} = L_{34}^2, \quad L_{46} = L_{10} L_5^2, \quad L_{47} = 2L_5 L_6 L_{10} + L_{11} L_5^2, \\
L_{48} &= 2L_5 L_6 L_{11} + L_{12} L_5^2 + L_6^2 L_{10}, \quad L_{49} = L_{11} L_6^2 + 2L_5 L_6 L_{12} + L_{13} L_5^2, \quad L_{50} = L_{12} L_6^2 + 2L_5 L_6 L_{13} + L_{14} L_5^2, \\
L_{51} &= 2L_5 L_6 L_{14} + L_{13} L_6^2, \quad L_{52} = L_{14} L_6^2, \\
R_1 &= E_c P_r L_{35}, \quad R_2 = -E_c P_r L_{36}, \quad R_3 = -E_c P_r L_{37}, \quad R_4 = -E_c P_r L_{38}, \quad R_5 = -E_c P_r L_{39} + E_c P_r L_{46}, \\
R_6 &= -E_c P_r L_{40} + E_c P_r L_{47}, \quad R_7 = -E_c P_r L_{41} + E_c P_r L_{48}, \quad R_8 = -E_c P_r L_{42} + E_c P_r L_{49}, \\
R_9 &= -E_c P_r L_{43} + E_c P_r L_{50}, \quad R_{10} = -E_c P_r L_{44} + E_c P_r L_{51}, \quad R_{11} = -E_c P_r L_{45} + E_c P_r L_{52}, \\
R_{12} &= \frac{R_1}{132}, \quad R_{13} = \frac{R_2}{110}, \quad R_{14} = \frac{R_3}{90}, \quad R_{15} = \frac{R_4}{72}, \quad R_{16} = \frac{R_5}{56}, \quad R_{17} = \frac{R_6}{42}, \quad R_{18} = \frac{R_7}{30}, \quad R_{19} = \frac{R_8}{20}, \\
R_{20} &= \frac{R_9}{12}, \quad R_{21} = \frac{R_{10}}{6}, \quad R_{22} = \frac{R_{11}}{2}, \\
R_{23} &= R_{12} h_1^{12} + R_{13} h_1^{11} + R_{14} h_1^{10} + R_{15} h_1^9 + R_{16} h_1^8 + R_{17} h_1^7 + R_{18} h_1^6 + R_{19} h_1^5 + R_{20} h_1^4 + R_{21} h_1^3 + R_{22} h_1^2, \\
R_{24} &= R_{12} h_2^{12} + R_{13} h_2^{11} + R_{14} h_2^{10} + R_{15} h_2^9 + R_{16} h_2^8 + R_{17} h_2^7 + R_{18} h_2^6 + R_{19} h_2^5 + R_{20} h_2^4 + R_{21} h_2^3 + R_{22} h_2^2, \\
R_{25} &= \frac{R_{24} - R_{23}}{h_1 - h_2}, \quad R_{26} = -R_{23} - R_{25} h_1, \quad R_{27} = 7 + 6E_c P_r, \quad R_{28} = (7 + 18E_c P_r) q_0, \quad R_{29} = E_c P_r q_0^3, \\
R_{30} &= 6E_c P_r q_0^3.
\end{aligned}$$

- [1] T. Hayat, N. Ahmed, and N. Ali, *Commun. Nonlinear Sci. Numer. Simul.* **13**, 1581 (2008).
- [2] M. Kothandapani and S. Srinivas, *Int. J. Nonlinear Mech.* **43**, 915 (2008).
- [3] A. H. Abd El-Naby and A. E. M. El-Misiery, *Appl. Math. Comput.* **128**, 19 (2002).
- [4] M. Li and J. G. Brasseur, *J. Fluid Mech.* **248**, 129 (1993).
- [5] J. C. Misra and S. K. Pandey, *Appl. Math. Comput.* **33**, 997 (2001).
- [6] L. M. Srivastava and V. P. Srivastava, *J. Biomech.* **17**, 821 (1982).
- [7] T. Hayat, M. U. Qureshi, and Q. Hussain, *Appl. Math. Modelling* **33**, 1862 (2009).
- [8] G. Radhakrishnamacharya and Ch. Srinivasulu, *C. R. Mecanique* **335**, 369 (2007).
- [9] K. Vajravelu, G. Radhakrishnamacharya, and V. Radhakrishnamurthy, *Int. J. Nonlinear Mech.* **42**, 754 (2007).
- [10] S. Nadeem and N. S. Akbar, *Commun. Nonlinear Sci. Numer. Simul.* **14**, 4100 (2009).
- [11] T. Hayat and N. Ali, *Commun. Nonlinear Sci. Numer. Simul.* **13**, 1343 (2008).
- [12] S. Srinivas and M. Kothandapani, *Appl. Math. Comput.* **213**, 197 (2009).
- [13] N. Ali, Q. Hussain, T. Hayat, and S. Asghar, *Phys. A* **372**, 1477 (2008).
- [14] A. El. Hakeem, A. E. I. Naby, A. E. M. El. Misery, and I. I. El Shamy, *J. Phys. A* **36**, 8535 (2003).
- [15] E. F. Elshehawey and Z. M. Gharsseldien, *Appl. Math. Comput.* **153**, 417 (2004).
- [16] A. M. Hakeem, A. El. Naby, A. E. M. El. Misery, and I. I. El Shamy, *Appl. Math. Comput* **158**, 497 (2004).
- [17] A. M. El. Misery, A. El. Hakeem, A. El. Naby, and A. H. El. Nagar, **72**, 89 (2001).
- [18] S. Srinivas and M. Kothandapani, *Int. Com. Heat and Mass Trans.* **35**, 514 (2008).

- [19] G. Radhakrishnamacharya and V. R. Murthy, *Def. Sci. J.* **43**, 275 (1993).
- [20] Kh. S. Mekheimer and Y. Abd Elmaboud, *Phys. A* **372**, 1657 (2008).
- [21] M. Massoudi and I. Christie, *Int. J. Nonlinear Mech.* **30**, 687 (1995).
- [22] A. Pantokratoras, *Int. J. Thermal Sci.* **45**, 378 (2006).
- [23] S. Nadeem and M. Ali, *Commun. Nonlinear Sci. Numer. Simul.* **14**, 2073 (2009).
- [24] S. Nadeem, N. S. Akbar, *Commun. Nonlinear Sci. Numer. Simul.* **14**, 3844 (2009).
- [25] S. Nadeem, T. Hayat, N. S. Akbar, and M. Y. Malik, *Int. J. Heat Mass Transfer* **52**, 4722 (2009).